Temperature-Dependent Selective Crystallization Behavior of Isotactic Polypropylene with a β-Nucleating Agent

Ziwei Cai,[1] Yao Zhang,[1] Jingqing Li,[1] Yingrui Shang,[1] Hong Huo,[2] Jiachun Feng,[3] Sergio S. Funari,[4] Shichun Jiang[1]

[1]School of Materials Science and Engineering, Tianjin University, Tianjin 300072, People's Republic of China
[2]Institute of Polymer Chemistry and Physics, College of Chemistry, Beijing Normal University, Beijing 100875, People's Republic of China
[3]Key Laboratory of Molecular Engineering of Polymers of Ministry of Education, Department of Macromolecular Science and Laboratory of Advanced Materials, Fudan University, Shanghai 200433, People's Republic of China
[4]Hamburger Synchrotronstrahlungslabor, Deutsches Elektronen-Synchrotron, Notkestraße 85, D-22607 Hamburg, Germany
Correspondence to: S. Jiang (E-mail: scjiang@tju.edu.cn)

ABSTRACT: The crystallization behavior of isotactic polypropylene (iPP) induced with various concentrations of the β-form nucleating agent aryl amide derivative (TMB-5) at different temperatures was investigated with synchrotron small-angle X-ray scattering and wide-angle X-ray scattering (WAXS) and polarized optical microscopy. The WAXS results indicate that TMB-5 is a temperature-dependent selective nucleating agent for iPP crystallization. This means that only β crystals or α crystals form at low or high crystallization temperatures, respectively; both β and α crystals can be found at a suitable crystallization temperature. A mechanism was proposed to understand this phenomenon and the crystallization behavior of iPP with the nucleating agent. © 2012 Wiley Periodicals, Inc. J. Appl. Polym. Sci. 000: 000–000, 2012

INTRODUCTION

The applicable properties of crystalline polymers are determined by their final formed structures and the process of structure formation. The processing and structure of crystalline polymers have attracted the interest of researchers because of its promising performances. Isotactic polypropylene (iPP) is one of the most commonly used semicrystalline polymers; it can form several crystal modifications: monoclinic (α), trigonal (β), and orthorhombic (γ) form and the smectic mesophase.[1–3] The α phase is the dominant crystal modification when the polymer material solidifies from the meld under ordinary conditions. The β form is usually induced by flow or β-nucleating agents. The γ form is formed preferentially under pressure.[4] Under certain conditions, for example, during undercooling, a mesophase, usually referred to as *smectic*, is formed instead of a crystalline phase.[5]

In past decades, numerous research groups have dedicated considerable efforts to the preparation of the β-modified iPP (β-iPP) because of its excellent mechanical properties. Varga et al.[6,7] reported differences in the physical properties between the α and β forms of iPP. It has been reported that in a comparison to the β

form, the α form showed a higher modulus and tensile strength and inferior fracture toughness. The impact strength and toughness of β-iPP exceeded those of α-iPP. The improved mechanical performance of β-iPP makes it very attractive for numerous applications.[8,9] The production of β-iPP requires the presence of β-nucleating agents, which have a high activity, selectivity, and sufficient physical and chemical stabilities. The amount of β crystals might be increased under some special conditions, such as shearing[10–12] or elongation[13] of the melt during crystallization, directional crystallization in a temperature-gradient field,[14] quenching of the melt to a certain temperature range, vibration-induced crystallization,[15] and addition of nucleating agents into the sample.[7,16] Although the implementation of efficient and selective β nucleants is the most reliable method for the preparation of samples rich in β modification, Varga et al.[17] demonstrated that calcium pimelate and suberate have the highest selectivity among all known β-nucleating agents.

It is known that specific crystals can be induced by the addition of specific nucleating agents (α- or β-nucleating agent in the case of iPP).[18–22] However, this method is too complex and
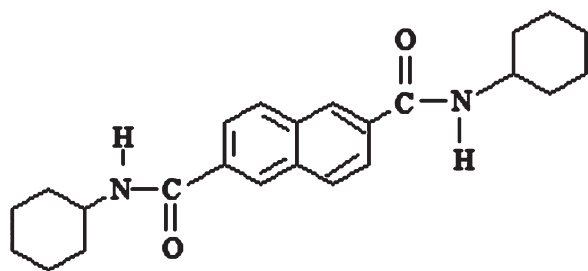
Figure 1. Chemical structure of N,N'-dicyclohexyl-2,6-naphthalene dicarboxamide.

difficult to manipulate for commercial products. The selective nucleating agent is attractive for obtaining ideal materials of iPP with designed proportional α and β form crystals via a simple and convenient approach. In this study, an aryl amide derivative (TMB-5) was used as nuclei for iPP crystallization. TMB-5 has been reported as a nonselective nucleating agent for iPP, with a melting point of 197°C. Both α- and β-iPP can be found in the presence of TMB-5. This behavior of TMB-5 is termed as a *dual nucleating ability.*[23] TMB-5 is an aromatic amide derivative with similar chemical structures to some aromatic amine β-nucleating agents. Although temperature-related studies on similar nucleating agents and iPP systems have been done by some other researchers with good results,[24–27] our results have great industrial interest. Our detailed study, related to the dual nucleation of TMB-5, indicated that it is a temperature-dependent selective nucleating agent for iPP crystallization. The wide-angle X-ray scattering (WAXS) results indicated that only β crystals or α crystals formed at low or high crystallization temperatures, respectively; both β and α crystals could be found at the proper crystallization temperature. Taking advantage of this excellent feature, we adjusted the temperature to get the kind of iPP that we wanted.

EXPERIMENTAL

Materials

The iPP used in this study was a commercial product of Aldrich Chemical Co., Inc. (Washington, WI 53074 US). The weight- and number-average molecular weights were 3.4×10^5 and 7.4×10^4 g/mol, respectively, measured by gel permeation chromatography. The melting point of iPP was around 165°C. TMB-5 was supplied by the Chemical Institute of Shanxi, China. Unfortunately, we are not aware of any corresponding work on the chemical structure and crystal information of TMB-5 on the basis of the relevant patent. As far as we know, it is an aromatic amide derivative with similar chemical structures to some aromatic amine β-nucleating agents, such as N,N'-dicyclohexyl-2,6-naphthalene dicarboxamide. The chemical structure according to ref.[26] is shown in Figure 1.

Sample Preparation

iPP granules and TMB-5 powder were put into the 60-mL chamber of an XSS-300 torque rheometer (Shanghai, China) together and melt-mixed at 190°C for 10 min at a rotation speed of 30 rpm. The obtained iPP/TMB-5 blends were soon sampled and then molded into 1 mm thick sheets. The concentrations of the nucleating agent were 0.05, 0.1, 0.2, 0.5, and 1 wt %, and the samples were designated as PP1, PP2, PP3, PP4, and PP5,

respectively. The pure iPP sample, designated as PP0, was prepared in an identical process for comparison.

Synchrotron Small-angle X-ray Scattering (SAXS) and WAXS Measurements

X-ray scattering experiments were performed with synchrotron radiation at $\lambda = 0.150$ nm on a Beamline A2 at Hamburger Synchrotronstrahlungslabor (Hamburg, Germany) for simultaneous SAXS/WAXS measurements and $\lambda = 0.154$ nm on a Beamline 4B9A at the Beijing Synchrotron Radiation Facility (Beijing, China) for WAXS measurements with a Mar165 charged coupling device detector (Hamburg, Germany). Two linear position-sensitive detectors were used, with one of them covering the approximate 2θ range from 10 to 30° and the other being set at a 230-cm sample–detector distance in the direction of the beam on the A2. The aluminum-foil-packed samples for *in situ* synchrotron investigation were heated to 220°C and kept there for 5 min to eliminate the thermal history before they were cooled down to their isothermal crystallization temperatures as soon as possible with the temperature controller on the Beamline A2. The cooling rate was 30°C/min with a Linkam heat stage on the Beamline 4B9A. The synchrotron SAXS/WAXS data were recorded as soon as the temperatures cooled down to the isothermal crystallization temperatures.

Polarized Optical Microscopy (POM)

An Olympus POM (TH4-200, Japan) equipped with a Q-imaging color video camera and a Linkam optical high-temperature stage (TST 350, United Kingdom) was used to observe the crystallization morphology in the isothermal crystallization progress of iPP/TMB-5 blends. Films of iPP containing TMB-5 of about 10 μm thickness were prepared for POM. The prepared samples for POM observation were heated to 220°C on the hot stage at a ramping rate of 30°C/min and then kept at 220°C for 5 min to eliminate the thermal history before they were cooled down to 25, 135, 140, 145, and 150°C for isothermal crystallization at the rate of 30°C/min. The final morphologies of the isothermally crystallized samples were observed with POM and were recorded as POM images.

Evaluation of the β Modification

The relative amount of β modification could be estimated from the K values of the samples. The K value is a relative measure of the β content of iPP, and it is zero in the absence of the β form and unity when only the β form is present. The β content of iPP was evaluated by the method of Turner-Jones et al.,[28] as shown in eq. (1):

$$K = I(300)_\beta / [I(300)_\beta + I(110)_\alpha + I(040)_\alpha + I(130)_\alpha] \quad (1)$$

where $I(110)$, $I(040)$, and $I(130)$ are the intensities of three typical peaks of the α form attributed to the (110), (040), and (130) planes of α cell, respectively. Although $I(300)$ is the intensity of the strongest diffraction peak of the β form, the K value is a relative measure of the β content of iPP, and it is zero in the absence of the β form and unity when only the β form is present.

RESULTS AND DISCUSSION

To measure the β-phase content in crystallized iPP samples, the WAXS profiles were analyzed, and the relative fractions of β-iPP were obtained. Figure 2 shows the WAXS profiles of the iPP/
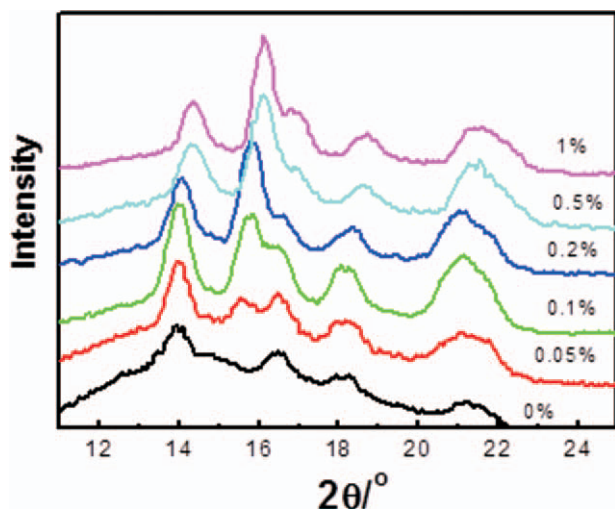
Figure 2. WAXD patterns of sample PP0 (pure iPP) and nucleated iPP with different TMB-5 contents at room temperature under quiescent conditions. [Color figure can be viewed in the online issue, which is available at wileyonlinelibrary.com.]

TMB-5 blends with various TMB-5 concentrations crystallized at room temperature. It was observed that the WAXS profile of pure iPP showed four obvious peaks at 2θ values of 13.9, 16.5, 18.2, and 21.3°, which corresponded to the (110), (040), (130), and (131) diffractions, respectively. These characteristic diffraction peaks indicated that only the α-crystal form existed in the pure iPP sample. From the results in Figure 2, we can see that even at a low concentration of TMB-5 (0.05 wt %), there was an obvious peak at about 16°; this corresponded to the (300) diffraction of the β-crystal form and indicated that the β-crystal form existed in the samples. The diffraction intensity of the β-marker peak increased with the nucleating agent, as shown in Figure 2; this implied an the increase in the portion of the β phase and a decrease in the α-phase amount in the specimen. This result also shows that TMB-5 was an effective nucleating agent for inducing iPP to form β crystals.

The understanding of iPP crystallization with a β-nucleating agent is important in both scientific research and commercial applications. However, the mechanism of the nucleating-agent-induced crystallization of β-iPP is still not well understood. The dimensional lattice matching theory proposed by Lotz et al.[29,30] has been widely accepted for some β-nucleating agents of iPP. The theory explains the β-iPP nucleating ability through analysis of the structural relationship between the nucleating agent and the β-form iPP. A lattice matching between the c-axis periodicity of iPP (6.5 Å) and the corresponding distance in the substrate crystal face of the nucleating agent is the main reason for the induction of the β-form iPP polymorph. The nucleating agents provide the nucleation surfaces for the iPP crystal. Kawai et al.[31] proposed the equation of the misfit factor (f_m) between the two crystal structures of iPP and the nucleating agent which can be calculated as follows:

$$f_m = (PB - PA)/PA \times 100\% \qquad (2)$$

where PA and PB are the appropriate period lengths of the substrate and polymer, respectively. When $f_m < 15\%$, the epitaxy is

considered to be good. The f_m value between the layer spacing of TMB-5 and the c axis of iPP is 2.9%; this indicated excellent epitaxy. According to Kawai et al.,[31] the c axis of the iPP aligned parallel to the b axis of the TMB-5. We concluded that the bc plane of the TMB-5 crystal was the epitaxial surface, onto which the (330) β plane of the β-phase iPP grew. Analysis of the molecular packing of the iPP helix onto the epitaxial surface determined in this study revealed that the β phase exhibited a good fit to this surface, whereas the α phase did not.

An analysis of the relationship between the polymeric nucleating agents and the β-crystal structure helps determine the structural requirements for the nucleating agent. The β modification of iPP has a β-unit cell with the parameters a = b = 1.101 nm and c = 0.65 nm and contains three isochiral helices. This cell is frustrated: the three helices do not have similar azimuthal orientations.[32] It does not comply with the rules of classical crystallography, which postulates structural equivalency. Different nucleating agents can induce these helical chains to organize into several different spatial arrangements and give rise to distinct polymorphs.[33]

It is known that the thermal history has an influence on the crystallization behavior and structure of crystalline polymers.[34–39] The changes in crystal forms between α and β for iPP have been studied by many researchers, and the difference in crystallization between the α and β forms is strongly related to the kinetics of the crystallization. For example, α-form crystals with β-nucleating agents are generated at higher crystallization temperatures, and the β form is crystallized at lower temperatures. α forms are generated again at crystallization temperatures below 80°C. These changes in the crystal forms could be related to the difference in the crystal growth rates of the α and β forms (G_α and G_β, respectively) at each crystallization temperature. Therefore, we tracked the TMB-5 induced isothermal crystallization process of iPP with synchrotron SAXS/WAXS measurements. The WAXS profiles of the iPP/TMB-5 blends with different TMB-5 contents isothermally crystallized at 135 and 140°C were obtained, and the final results of the samples are shown in Figure 3. From the results shown in Figure 3(a), we observed that when the concentration of TMB-5 was below 0.2 wt %, only the typical peaks of β crystals at about 15.8° were visible. The peak at 2θ of approximately 14.0°, which corresponded to the (110) diffraction for the α crystal, was observed when the nucleating agent content was higher than 0.2%. However, the intensity of this peak was very faint. From the results in Figure 3(b), we observed that the intensity of the β form crystal diffraction increased with the concentration of the nucleating agent; this indicated that the β crystals increased with the nucleating agent. This figure also shows that at a low concentration of nucleating agent (0.05 wt %), there were visible peaks at about 14.0, 16.5, and 18.2°, which corresponded to the (110), (040), and (130) diffractions, respectively, of the α-crystal form. This indicated the existence of the α-crystal form in the investigated sample. In iPP6 [iPP/TMB-5 (1 wt %)], the β-nucleating agent provided a large amount of heterogeneous nucleation sites for the growth of β crystals, so the typical diffraction characteristic of the β-iPP modification was clearly observed. Meanwhile, relatively low-intensity diffraction peaks, which corresponded to the α crystals of iPP, were observed in the same profile.
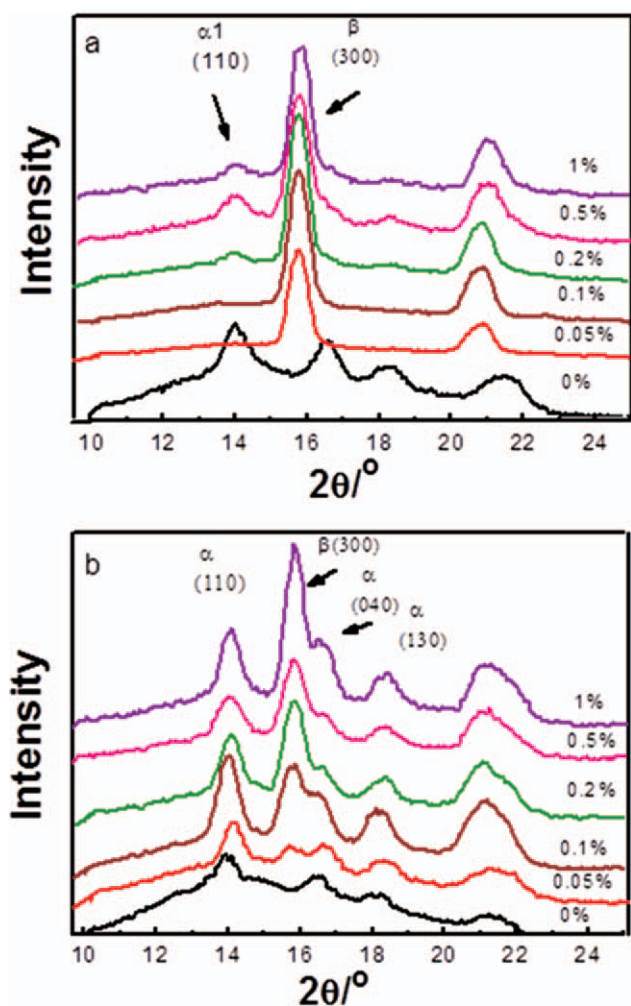
Figure 3. WAXD patterns of sample PP0 (pure iPP) and nucleated iPP with different TMB-5 contents crystallized at (a) 135 and (b) 140°C. [Color figure can be viewed in the online issue, which is available at wileyonlinelibrary.com.]

The crystallization of both the α and β forms at 140°C with TMB-5 were observed with WAXS. The crystalline morphology images with various nucleating agents obtained from POM are shown in Figure 4. It could be seen that the spherulite size of pure iPP (PP0) was larger than that of the iPP samples with TMB-5.

The spherulite growth in pure iPP was a nucleation-controlled homogeneous nucleation of crystallization. Therefore, the iPP spherulite grew very large before it impinged on another spherulite. Although in iPP with nucleating agent, a large number of nucleating sites were induced by the nucleating agent, the spherulite could not grow large enough to overlap, and the increased nucleus density resulted in a significant decrease in the average size of the spherulites.

The nucleation and growth mechanism were sensitive to the concentration of TMB-5, as discussed earlier, and caused a relative change (an increase in the numbers and a decrease in the size of spherulites) in the crystalline modification (Fig. 4) that

varied with the conditions adopted for the investigation. This was confirmed by the result of WAXS.

To determine the evolution of β crystals with a fixed crystallization temperature, the intensity of the β-marker peak from WAXS and SAXS as a function of the crystallization time are presented in Figure 5. As shown in Figure 5, the crystallization rate increased with the concentration of TMB-5. The intensity of the β peaks increased with time for samples with different TMB-5 concentrations. It turned out that the addition of the TMB-5 agent facilitated the formation of the β phase. On the other hand, the intensity became stable beyond a certain time. Meanwhile, the maximum intensity of the peaks of the β phase were identical for all of the samples; this implied that the increase in the TMB-5 composition in iPP did not affect the ratio of the β phase in the stable state of the crystallization.

Both α and β crystals are based on the same threefold helical conformation of the chain. The heat distortion temperature of the β phase exceeds that of α-iPP.[7] Therefore, β-iPP is a metastable phase (it melts at <155°C, as opposed to <170°C for α-iPP), and its growth rate is higher (by up to 70%) than that of α-iPP over most of the usual crystallization temperature range (i.e., 100–140°C). A high content of β-iPP can be obtained within this crystallization temperature range. The most favorable temperature for β-form growth is near 135°C. Therefore, when iPP/TMB-5 was crystallized at 135°C, the content of the β crystal form was high, and few α-crystal forms could be found in the sample. Crystallization is an exothermic process; thus, the value of enthalpy (ΔH) is negative. In comparison with that of α-iPP, the enthalpy of β-iPP (ΔH_β) is higher during the formation of the β form ($\Delta H_\alpha = 170$ J/g, $\Delta H_\beta = 168.5$ J/g).[7] Thermodynamically, the phase with a lower enthalpy is more favorable. Moreover, as reported by Varga et al.,[40] on account of the higher melting temperature, α-iPP grows faster than β-iPP at high temperatures and above a critical temperature ($T_c = 140$°C). Therefore, the crystallization of the metastable β-crystal form is slow at higher crystallization temperatures because of the lower supercooling temperature ($T_m - T_c$) and fusion enthalpy, whereas the α-form becomes more stable and kinetically favorable (T_m is the melting point). So the amount of α-crystal form increased with crystallization temperature in the iPP/TMB-5 systems, and it was reasonable to conclude that the crystalline temperature was a crucial element in the final crystallization structure of the iPP for iPP/TMB-5 systems.

It is known that the crystallization temperature influences the polymer crystallization behavior and structure of crystalline polymers. The nucleation and growth mechanism were very sensitive to the concentration of TMB-5. The content of the β phase increased with TMB-5 percentage, as shown in Figure 3. However, the peaks in the WAXS profile resulted from the α crystals of iPP and could be found, as shown in Figure 3(a), even when the crystallization temperature was 135°C with concentrations of TMB-5 higher than 0.2 wt %. Only β crystals of iPP could be induced, as shown in the WAXS profile [Fig. 3(a)], when the concentration of TMB-5 was lower than 0.2 wt %. This phenomenon was not consistent with reported results[24,26] because TMB-5 was considered as a β-nucleating agent. As shown in Figures 4 and 5, the numbers of spherulites
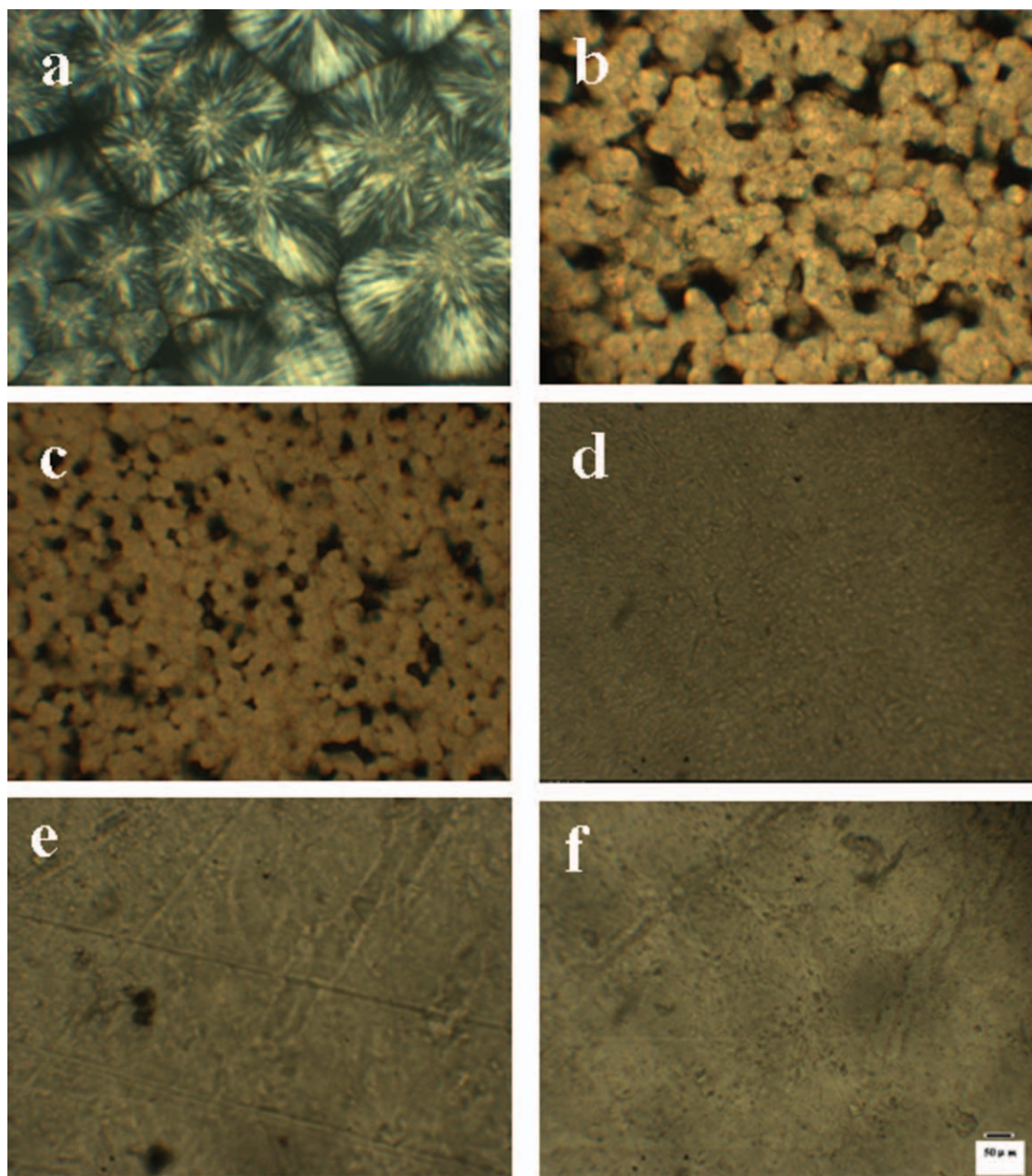
Figure 4. Micrographs of pure iPP and nucleated iPP samples crystallized at 135°C: (a) pure iPP and (b) 0.05, (c) 0.1, (d) 0.2, (e) 0.5, and (f) 1 wt % iPP. [Color figure can be viewed in the online issue, which is available at wileyonlinelibrary.com.]

and the rate of crystallization increased with the concentration of TMB-5. The crystallization process is an exothermic process. The increase in the number of spherulites originated from the increase of TMB-5 induced nucleating sites and led to increases in the crystallization rate and exothermic heat. The exothermic heat, which cannot be spread out in time, led to an increase the local crystallization temperature. Nakamura et al.[41] studied G_α and G_β over a wide range of crystallization temperatures. They indicated that the ratio of crystal growth rates (G_β/G_α) varied with the crystallization temperature. The intersection of the crystal growth rate from β to α form ($G_\alpha > G_\beta$) was observed at about 140°C. On the other hand, in the temperature range

below 105°C, it was predicted that G_α became faster again than G_β. These crossover temperatures may have been different with a difference in isotacticity. This phenomenon was first reported by Varga.[42] So the increase in the local crystallization temperature could promote G_α, and this resulted in the formation of α crystals. In addition, the crystal density increased with nucleating sites, and then, the interaction between spherulites increased in a fixed volume. The densities of the α and β phases were 0.949 and 0.939 g/cm³, respectively, according to the close match of the melting temperatures of the corresponding crystalline phases with those in the literature.[16] The increase in the crystal density was preferred to form the α phase because of the
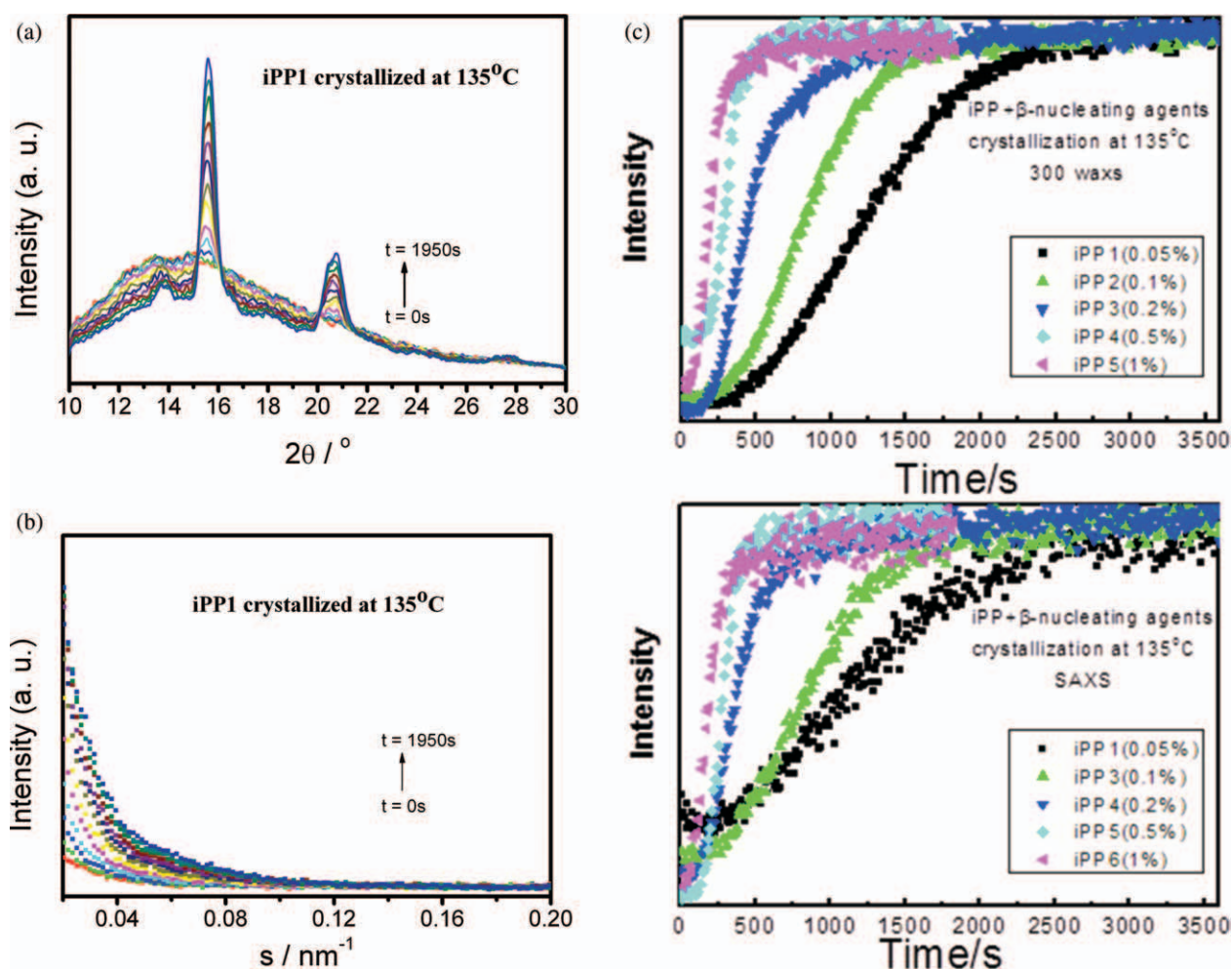
Figure 5. Time (*t*)-dependent scattering intensity values of samples isothermally crystallized at 135°C (WAXS and SAXS) simultaneously obtained from iPP1 crystallized at 135°C. WAXS: $2\theta = 15.8$ obtained from WAXS ($\lambda = 0.150$ nm) profiles. SAXS: $s = 0.046$ nm^{-1} obtained from SAXS ($\lambda = 0.150$ nm, $s = 2\sin\theta/\lambda = q/2\pi$) profiles. [Color figure can be viewed in the online issue, which is available at wileyonlinelibrary.com.]

greater density of the α phase. Therefore, we were convinced that the crystallization temperature was the dominant element for the TMB-5 induced iPP crystallization with selectivity. The phenomenon was confirmed by the final WAXS profiles of the iPP/TMB-5 blends isothermally crystallized at 135 and 140°C (Fig. 3), especially the results in Figure 7 (shown later for the samples crystallized at 145°C).

The relationship between the relative β content and the nucleating agent could be determined by the *K* value according to the WAXS results. Generally speaking, an increase in the concentration of the nucleating agent helps to increase the proportion of β crystals. The β-nucleating agent provided a large amount of heterogeneous nucleation sites for the growth of β crystals. The $K_\beta(300)$ values calculated by the WAXS data are plotted in Figure 6 as a function of the nucleating agent content. $K_\beta(300)$ is the content of the strongest diffraction peak of the trigonal β-form. From the results in Figure 6, we determined that the β form of the samples containing β-nucleating agent increased rapidly until the agent content was more than 0.2% and then

slightly increased with continuously increasing agent content. This showed a critical nucleation concentration. The dependence of the $K_\beta(300)$ values on the concentration of nucleating agent has been investigated by several researchers, and a similar trend has been observed.[33,43–45] To demonstrate the influence of the temperature on the nucleation of TMB-5, we investigated samples crystallized at higher temperatures via *in situ* synchrotron SAXS/WAXS measurements. Figure 7 shows the WAXD patterns of the nucleated iPP with different TMB-5 contents crystallized at 145°C. From the results shown in Figure 7, we observed that when the samples crystallized at 145°C, only the α-crystal form existed in the observed iPP sample; this was also different from those crystallized at 135 and 140°C.

TMB-5 is an effective β-form nucleating agent for iPP crystallization above a critical concentration, but it is not completely selective; a certain amount of α phase can be detected in all samples. This behavior of TMB-5 is termed as a *dual nucleating ability* and was confirmed by Varga et al.[40] in a previous work. Varga et al. proved that TMB-5 is not a selective β-nucleating agent

because of the partial α-nucleating effect of its lateral crystal surface. The α-nucleating effect was shown directly in their polarized light microscopy (PLM) micrographs. Therefore, it was suitable for use in the investigation of the crystallization and transition behaviors of iPP. However, according to our experimental results, TMB-5 was a temperature-dependent selective nucleating agent. TMB-5 played different roles in promoting the nucleation under different temperatures. When the iPP/TMB-5 blends crystallized at 135°C, TMB-5 only promoted the nucleation of the β phase; When the blends crystallized at 140°C, TMB-5 stimulated the nucleation of the β phase together with the α phase; When the temperature was above 140°C, TMB-5 only had a role in promoting the nucleation of the α phase. The reason for the temperature-dependent selective nucleating phenomenon we considered to be related to the thermodynamics and kinetics of the TMB-5 induced crystallization of iPP. It is known that both α and β crystals are based on the same threefold helical conformation of the polymer chain. The heat distortion temperature of the β phase exceeds that of α-iPP.[7] The growth rate of metastable β-iPP is higher (by up to 70%) than that of α-iPP over most of the usual crystallization temperature range (i.e., between 100 and 140°C), and 135°C is the most favorable temperature for the formation of the β form. Crystallization is an exothermic process with a negative enthalpy ($\Delta H_\alpha =$ 170 J/g; $\Delta H_\beta = 168.5$ J/g).[7] Thermodynamically, the α phase, with a lower enthalpy, is more favorable. Moreover, α-iPP grows faster than β-iPP at high temperatures on account of the supercooling temperature, especially above a T_c of 140°C. In addition, the increase of TMB-5 induced nucleating sites led to increases in the crystallization rate and exothermic heat. The exothermic heat, which cannot be spread out in time, led to a rise in the local crystallization temperature. Therefore, at higher crystallization temperatures, the crystallization of the metastable β-crystal form is slow because of its lower supercooling temperature and fusion enthalpy, whereas the α form becomes more stable and kinetically favorable. Therefore, the α-crystal form increases with the crystallization temperature in iPP/TMB-5 systems.
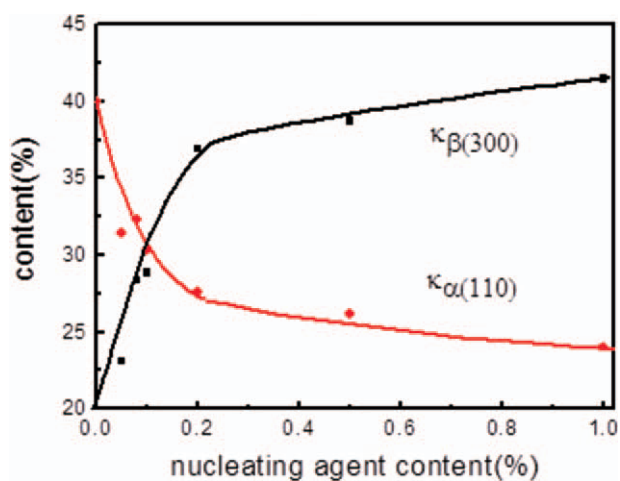

Figure 7. WAXD patterns of nucleated iPP samples with different TMB-5 contents crystallized at 145°C. [Color figure can be viewed in the online issue, which is available at wileyonlinelibrary.com.]

CONCLUSIONS

In this study, the nucleating ability of TMB-5 toward iPP and its effects on the content of β crystals and the crystallization behavior of iPP under an isothermal crystallization process were investigated. The experimental results indicate that TMB-5 is a temperature-dependent selective nucleating agent for iPP crystallization. In another words, only β crystals or α crystals formed at crystallization temperatures of 135 or 145°C, respectively; both β and α crystals could be found at 140°C. The changes in crystal forms were strongly related to the kinetics of crystallization. That is, at different crystallization temperatures with TMB-5, which is a temperature-dependent selective nucleating agent, the α and β forms had different crystal growth rates.

Figure 6. $K_\beta(300)$ and $K_\alpha(110)$ values as a function of the TMB-5 content. $K_\alpha(110)$ is the content of a typical peaks of α-form attributed to the (110) planes of monoclinic cell. [Color figure can be viewed in the online issue, which is available at wileyonlinelibrary.com.]
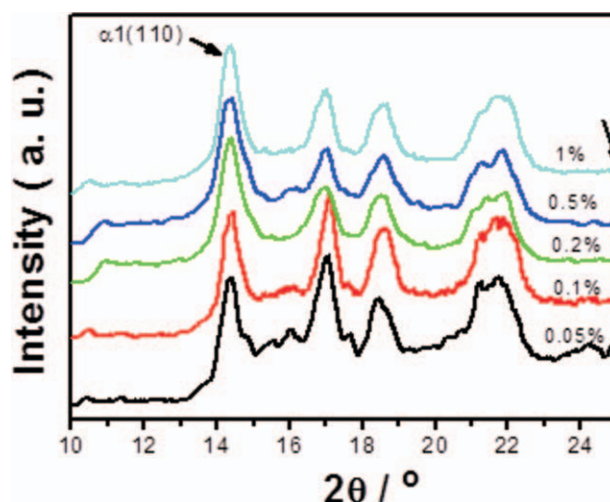
REFERENCES

1. Liu, M. X.; Guo, B. C.; Du, M. L.; Chen, F.; Jia, D. M. *Polymer* **2009,** *50,* 3022.

2. Menyhárd, A.; Gahleitner, M.; Varga, J.; Bernreitner, K.; Jääskeläinen, P.; Øysæd, H.; Pukánszky, B. *Eur. Polym. J.* **2009,** *45,* 3138.

3. Zhang, P. Y.; Liu, X. X.; Li, Y. Q. *Mater. Sci. Eng. A.* **2006,** *434,* 310.

4. Bruckner, S.; Phillips, P. J.; Mezghani, K.; Meille, S. V. *Macromol. Rapid. Commun.* **1997,** *18,* 1.

5. Lezak, E.; Bartczak, Z.; Galeski, A. *Polymer* **2006,** *47,* 8562.

6. Chen, H. B.; Karger-Kocsis, J.; Wu, J. S.; Varga, J. *Polymer* **2002,** *43,* 6505.

7. Varga, J. *J. Macromol. Sci. Phys.* **2002,** *41,* 1121.

8. Shangguan, Y. G.; Song, Y. H.; Peng, M.; Li, B. P.; Zheng, Q. *Eur. Polym. J.* **2005,** *41*, 1766.

9. Han, L.; Li, X. X.; Li, Y. L.; Huang, T.; Wang, Y.; Wu, J.; Xiang, F. M. *Mater. Sci. Eng, A.* **2010,** *527*, 3176.

10. Varga, J.; Karger-Kocsis, J. *J. Polym. Sci. Part. B: Polymer Phys. Ed.* **1996,** *34*, 657.

11. Somani, R. H.; Hsiao, B. S.; Nogales, A.; Fruitwala, H.; Srinivas, S.; Tsou, A. H. *Macromolecules* **2001,** *34*, 5902.

12. Chen, Y. H.; Mao, Y. M.; Li, Z. M.; Hsiao, B. S. *Macromolecules* **2010,** *43*, 6760.

13. Varga, J.; Ehrenstein, G. W. *Polymer* **1996,** *37*, 5959.

14. Lovinger, A. J.; Chua, J. O.; Gryte, C. C. *J. Polym. Sci. Polym. Phys. Ed.* **1977,** *15*, 641.

15. Zhang, J.; Shen, K.; Na, S.; Fu, Q. *J. Polym. Sci. Part. B: Polym. Phys.* **2004,** *42*, 2385.

16. Li, J. X.; Cheung, W. L. *Polymer* **1999,** *40*, 2085.

17. Menyhárd, A.; Varga, J.; Molnár, G. *J. Therm. Anal. Calorim.* **2006,** *83*, 625.

18. Romankiewicz, A.; Sterzynski, T.; Brostow, W. *Polym. Int.* **2004,** *53*, 2086.

19. Nezbedova, E.; Pospisil, V.; Bohaty, P.; Vlach, B. *Macromol. Symp.* **2001,** *170*, 349.

20. Cho, K.; Saheb, D. N.; Choi, J.; Yang, H. *Polymer* **2002,** *43*, 1407.

21. Yang, Z. G.; Mai, K. C. *J. Appl. Polym. Sci.* **2011,** *119*, 3566.

22. Qin, J.; Chen, X. L.; Yu, J.; Wang, Y.; Tian, Y. Z.; Wu, S. *J. Appl. Polym. Sci.* **2010,** *117*, 1047.

23. Varga, J.; Menyhárd, A. *Macromolecules* **2007,** *40*, 2422.

24. Dong, M.; Guo, Z. X.; Yu, J.; Su, Z. Q. *J. Polym. Sci. Part. B: Polym. Phys.* **2008,** *46*, 1725.

25. Dong, M.; Jia, M. Y.; Guo, Z. X.; Yu, J. *Chin. J. Polym. Sci.* **2011,** *29*, 308.

26. Dong, M.; Guo, Z. X.; Yu, J.; Su, Z. Q. *J. Polym. Sci. Part. B: Polym. Phys.* **2009,** *47*, 314.

27. Dong, M.; Guo, Z. X.; Su, Z.; Yu, J. *J. Appl. Polym. Sci.* **2011,** *119*, 1374.

28. Turner-Jones, A.; Aizlewood, J. M.; Beckett, D. R. *Macromol. Chem. Phys.* **1964,** *75*, 134.

29. Lotz, B. *Polymer* **1998,** *39*, 4561.

30. Mathieu, C.; Thierry, A.; Wittmann, J. C.; Lotz, B. *Polymer* **2000,** *41*, 7241.

31. Kawai, T.; Iijima, R.; Yamamoto, Y.; Kimura, T. *Polymer* **2002,** *43*, 7301.

32. Xu, W.; Martin, D. C.; Arruda, E. M. *Polymer* **2005,** *46*, 455.

33. Su, Z. Q.; Dong, M.; Guo, Z. X.; Yu, J. *Macromolecules* **2007,** *40*, 4217.

34. Yuan, Q.; Rajan, V. G.; Misra, R. D. K. *Mater. Sci. Eng. B.* **2008,** *153*, 88.

35. Medellin-Rodriguez, F. J.; Mata-Padilla, M.; Mata-Padilla, S.; Vega-Diaz, S.; Davalos-Montoya, O. *J. Polym. Sci. Part B: Polym. Phys.* **2008,** *46*, 2188.

36. Menyhárd, A.; Varga, J.; Liber, Á.; Belina, G. *Eur. Polym. J.* **2005,** *41*, 669.

37. Li, X. X.; Wu, H. Y.; Wang, Y.; Bai, H. W.; Liu, L.; Huang, T. *Mater. Sci. Eng. A.* **2010,** *527*, 531.

38. Menyhárd, A.; Varga, J. *Eur. Polym. J.* **2006,** *42*, 3257.

39. Yang, Z. G.; Zhang, Z. S.; Tao, Y. Z.; Mai, K. C. *J. Appl. Polym. Sci.* **2009,** *112*, 1.

40. Varga, J.; Mudra, I.; Ehrenstein, G. W. *J. Therm. Anal. Calorim.* **1999,** *56*, 1047.

41. Nakamura, K.; Satoko, S.; Umemoto, S.; Thierry, A.; Lotz, B.; Okui, N. *Polym. J.* **2008,** *40*, 915.

42. Varga, J. *J. Mater. Sci.* **1992,** *27*, 2557.

43. Zhao, S. C.; Cai, Z.; Xin, Z. *Polymer* **2008,** *49*, 2745.

44. Huo, H.; Jiang, S. C.; An, L. J. *Macromolecules* **2004,** *37*, 2478.

45. Xiao, W. C.; Wu, P. Y.; Feng, J. C. *J. Appl. Polym. Sci.* **2008,** *108*, 3370.